On the Ionization Energies of C_4H_3 Isomers

Ralf I. Kaiser,[a] Alexander Mebel,[b] Oleg Kostko,[c] Musahid Ahmed[c]

[a] Prof. R.I. Kaiser
University of Hawaii at Manoa, Department of Chemistry
Honolulu, HI 96822 (USA)

[b] Prof. A.M. Mebel
Florida International University, Department of Chemistry
Miami, 33199 (USA)

[c] Dr. O. Kostko, Dr. M. Ahmed
Chemical Sciences Division, Lawrence Berkeley National Laboratory
Berkeley, California 94720 (USA)

Abstract

We have conducted a combined experimental and theoretical study on the formation of distinct isomers of resonantly stabilized free radicals, C_4H_3, which are important intermediates in the formation of polycyclic aromatic hydrocarbons in combustion flames and possibly in the interstellar medium. Our study utilized laser ablation of graphite in combination with seeding the ablated species in neat methylacetylene gas which also acted as a reagent. Photoionization efficiency (PIE) curves were recorded of the C_4H_3 isomers at the Advanced Light Source from 8.0 to 10.3 eV. The experimental PIE curve was compared with theoretical ones suggesting the formation of four C_4H_3 radicals: two acyclic structures i-C_4H_3 [**1**] and E/Z-n-C_4H_3 [**2E/2Z**] and two cyclic isomers **3** and **4**. These molecules are likely formed via an initial addition of ground state carbon atoms to the carbon-carbon triple bond of the methylacetylene molecule followed by isomerization via hydrogen migrations and ring opening and emission of atomic hydrogen from these intermediates.

1. Introduction

Resonantly stabilized free radicals such as propargyl (C_3H_3; $HCCCH_2$; X^2B_1) and 1-buten-3-yn-2-yl (C_4H_3; $HCCCCH_2$; X^2A'), in which the unpaired electron is delocalized across the carbon skeleton, are considered as central reaction intermediates to form polycyclic aromatic hydrocarbons (PAHs) in combustion flames [1,2,3] and in the interstellar medium [4,5]. Whereas it is well established that the propargyl radical presents an exclusive open shell isomer among the C_3H_3 radicals detected in hydrocarbon flames [6,7,8], the situation is far from being resolved for the C_4H_3 radicals. The photo ionization curves, i.e. a plot of the ionization energy versus the count rates of the C_4H_3 ion at m/z = 51 was measured from analysis of propyne and allene flames photoionized with tunable VUV synchrotron radiation. These studies suggested the existence of at least a i-C_4H_3 isomer [9], which is thermodynamically favorable by 44 ± 2 $kJmol^{-1}$ compared to the n-C_4H_3 structure [10]. An adiabatic ionization energy (AIE) of 8.06 ± 0.05 eV was derived for the i-C_4H_3 isomer. Because of low Franck-Condon factors, the authors suggested that their sensitivity with respect to the n-C_4H_3 isomer was limited. Chemical dynamics experiments exploiting the crossed molecular beam method showed that C_4H_3 radicals can be formed under single collision conditions as a product of bimolecular reactions. These involve reactions of ground state carbon atoms ($C(^3P_j)$) with methylacetylene (CH_3CCH) [11] and allene (H_2CCCH_2) [12] as well as bimolecular collisions of dicarbon in its ground and first electronically excited states, i.e. $C_2(X^1\Sigma_g^+)$ and $C_2(a^3\Pi_u)$, with ethylene (H_2CCH_2); these processes lead to the synthesis of the C_s symmetric i-C_4H_3 isomer: $HCCCCH_2(X^2A')$. The n-C_4H_3 isomer (HCCCHCH; X^2A') was identified as a reactive intermediate formed in the initial addition of the ethynyl radical (CCH) to acetylene (HCCH). However, a detailed analysis of the center-of-mass functions as extracted from the crossed beam reactions of ground state carbon atoms with methylacetylene [11] suggested that an elusive high-energy isomer, might have also been synthesized. The molecular structure of this isomer is still unknown.

Which approach could be applied to unravel the structure of potential high-energy C_4H_3 isomers? For distinct structural isomers, the AIE can differ significantly [9]. Here, the AIE presents a measurable quantity of the energy required to remove an electron from a molecule in its rotational, vibrational, and electronic ground state hence forming a cation in its lowest electronic, vibrational, and rotational level. The AIE presents one of the most relevant thermochemical measurements:

ionization energies cannot only be utilized to determine the nature of the structural isomers, i.e. of hydrocarbon radicals, but they can be combined with thermochemical cycles to obtain enthalpies of formation of hydrocarbon radicals. Single photon ionization with tunable vacuum ultraviolet (VUV) radiation allows for the determination of AIE's of highly reactive organic transient radicals like linear and cyclic C_3H to be 9.15 eV and 9.76 eV, respectively [13]. Here, we synthesize multiple C_4H_3 isomers in a supersonic molecular beam via laser ablation of a graphite rod followed by *in situ* reaction of the ablated carbon atoms with methylacetylene. The neutral radicals in this supersonic beam are then photoionized by VUV light from the Advanced Light Source at various photon energies. Based on electronic structure calculations, the recorded photoionization efficiency curves are then simulated theoretically to extract the AIE's of the C_4H_3 isomers.

2. Theoretical Methods

Geometries of various C_4H_3 isomers and their ions have been optimized using the hybrid density functional B3LYP method [14,15] with the 6-311G** basis set. In general, this approach is known to be reliable for geometric parameters. For example, the bond lengths and bond angles optimized at the B3LYP/6-311G** level for *Z*-*n*-C_4H_3 and *E*-*n*-C_4H_3 coincide with those obtained by Wheeler et al. [16] by more sophisticated CCSD(T)/TZ(2*d*1*f*,2*p*1*d*) calculations within 0.01 Å and 1°, respectively. However, the *i*-C_4H_3 isomer is an exception. B3LYP calculations generates a C_{2v}-symmetric structure with a linear C_4 fragment for this isomer, contrary to the results of higher level calculations [17]. Therefore, we used the CCSD(T)/6-311G** optimized C_s-symmetric geometry for *i*-C_4H_3, which again is in close agreement with the CCSD(T)/TZ(2*d*1*f*,2*p*1*d*) results of Wheeler et al. [16]. For consistency, geometry of the *i*-$C_4H_3^+$ cation was also optimized at the CCSD(T)/6-311G** level; however, in this case the CCSD(T) and B3LYP geometries are very close. Vibrational frequencies were computed at B3LYP/6-311G**, except for *i*-C_4H_3 and its cation, for which the CCSD(T)/6-311G** method was employed. To refine vertical and adiabatic ionization energies of various C_4H_3 isomers, we performed coupled cluster CCSD(T) calculations [18] with extrapolation to the complete basis set (CBS) limit. To achieve this, we computed CCSD(T) total energies for each neutral and cationic C_4H_3 species with Dunning's correlation-consistent cc-pVDZ, cc-pVTZ, cc-pVQZ, and cc-pV5Z basis sets [19] and projected them to CCSD(T)/CBS total energies by fitting the following equation [20]

(1) $$E_{tot}(x) = E_{tot}(\infty) + Be^{-Cx}$$

where x is the cardinal number of the basis set (2, 3, 4, and 5, respectively) and $E_{tot}(\infty)$ is the CCSD(T)/CBS total energy. All ab initio calculations were carried out using the GAUSSIAN 98 [21] and MOLPRO 2006 [22] program packages. Franck-Condon factors calculations for the C_4H_3 ionization processes have been performed in harmonic approximation using a model of displaced and distorted harmonic oscillators [23,24] and utilizing molecular structures and vibrational frequencies of the neutral and ion species obtained from the ab initio calculations.

3. Experimental Methods

The experiments were conducted at the Chemical Dynamics Beamline of the Advanced Light Source at Lawrence Berkeley National Laboratory. The C_4H_3 isomers were formed *in situ* within a laser ablation source [13]. Here, about 2 mJ of the 532 nm output of a Neodymium-Yttrium-Aluminum-Garnet (Nd:YAG) laser were focused to a 1 mm spot onto a rotating graphite rod (99.995 %, Aldrich). The ablated species were then seeded in methylacetylene (99+ %; Aldrich) carrier gas, which was released by a Proch–Trickl pulsed valve operating at a stagnation pressure of 135 kPa and repetition rate of 50 Hz. The methylacetylene carrier gas also acted as a reactant to form multiple C_4H_3 radicals *in situ*. Tunable VUV light from the Advanced Light Source crossed the neutral molecular beam 120 mm downstream of the ablation center and 65 mm after the skimmer in the extraction region of a Wiley–McLaren reflectron time-of-flight (TOF) mass spectrometer. The ions of the photoionized molecules were extracted and collected by a microchannel plate detector in the reflectron mode utilizing a multi channel scaler. The photoionization efficiency (PIE) curves can be obtained by plotting the integrated $C_4H_3^+$ signal at mass-to-charge, m/z, of 51 versus the photoionization energy between 8.0 eV and 10.3 eV in steps of 0.1 eV. The signal was normalized to the photon flux. These PIE curves can be exploited to extract the adiabatic ionization energies of the radicals [13].

4. Results and Discussion

First, we would like to comment on the structures of low lying C_4H_3 isomers together with their cations. Hereafter, the ionization energies are discussed to aid an interpretation of the photoionization curve obtained for the C_4H_3 ions at m/z = 51. The optimized geometries of the neutral C_4H_3 isomers and their cations in the lowest singlet and triplet states are illustrated in Figure 1. For the present consideration, we have chosen five lowest energy C_4H_3 structures [17], *i*-C_4H_3 **1**, *E* and *Z* conformations of *n*-C_4H_3 **2E** and **2Z**, as well as two cyclic isomers **3** and **4**. *i*-C_4H_3 **1** represents the most stable structure, with *n*-C_4H_3 conformers residing ~0.5 eV higher in energy and **3** and **4** being 1.32 and 1.42 eV less favorable than **1**, respectively. Note that the energy difference between *i*-C_4H_3 and *n*-C_4H_3 calculated here closely matches the previous high-level results by Wheeler et al. [16] and Hansen et al. [9]. Ionization of **1** is found to significantly change its geometry. In particular, the symmetry of the molecule increases from C_s to C_{2v} as the C_4 chain becomes linear in the ion, both in the singlet (**1s**$^+$) and (**1t**$^+$) triplet electronic states. Since the singlet $^1A_1$ electronic state is much lower in energy than triplet $^3A_2$ (Table 1), we performed Franck-Condon factor calculations for $^1A_1$. The geometry relaxation in **1s**$^+$ as compared to **1** involves shortening of some C-C bonds by up to 0.03 Å, whereas CCC angles increase by up to 30°. These changes are reflected in significant displacements of several vibrational normal modes, which in turn result in small Franck-Condon factors with ionization peaks spread over a broad energy range (see Supporting Information). The calculated AIE, 8.01 eV, is 0.45 eV lower than the vertical ionization energy (VIE) (Table 1) and the ionization spectrum of **1** is predicted to represent a broad continuum originated at ~8 eV with slowly increasing intensity that can be spread as far as to the 10-11 eV energy range.

Although the *n*-C_4H_3 structures have VIEs to singlet ionic states slightly lower than those to the triplet states of the ion, the geometry relaxation in singlets is drastic; the **2Es**$^+$ and **2Zs**$^+$ structures optimize to C_{2v}-symmetric H_2CCCCH^+ (**1s**$^+$) and cyclic **4s**$^+$, respectively, starting from the equilibrium geometries of the neutral species. This means that Franck-Condon factors for ionization of *n*-C_4H_3 to singlet ionic states should be unfavorable. On the other hand, ionization to the triplet ionic states results in relatively minor geometric changes and is expected to give rise to short series of distinct peaks in the spectra. As seen in Table 1 and in Supporting Information, the series of ionization peaks due to **2Et**$^+$(^{3}A") ← **2E**(^{2}A') and **2Zt**$^+$(^{3}A") ← **2Z**(^{2}A') starts at ~9.7 eV and is

spread to ~10.2 eV, with the origin peaks being the most intense. The cyclic C_4H_3 isomer **3** at the vertical geometry has a ground triplet ^{3}A" ionic state, whereas the singlet ^{1}A' state is 0.45 eV higher in energy. Geometry relaxation of the singlet ion leads to the linear **1s$^+$** structure, which should result in very unfavorable Franck-Condon factors. Alternatively, geometry changes from **3** to the triplet **3t$^+$** ion are rather moderate and Franck Condon factor calculations give a series of distinct peaks with the origin at 8.67 and spreading over to ~9.9 eV (Supporting Information); the ionization peaks at 8.67 and 9.07 eV are predicted to be the most intense. The second cyclic isomer **4** has VIEs of 8.25 and 8.57 eV to singlet and triplet states, respectively. Geometry relaxation in the singlet state is more significant as the symmetry changes from C_s to C_{2v} with the out-of-ring CCH group becoming linear. Similar to **1**, we can expect the **4s$^+$** ← **4** ionization spectra to be a broad featureless continuum with the origin at 7.39 eV. Ionization to the triplet state, **4t$^+$**(^{3}A") ← **4**(^{2}A'), leads to moderate structural changes and the calculated Franck-Condon factors show a progression of separate ionization peaks, where the intensity of the origin peak at 8.21 eV by far exceeds intensities of the others.

Table 1. Calculated vertical and adiabatic ionization energies (in eV) of various C_4H_3 isomers.

	i-C_4H_3, **1**		*E*-*n*-C_4H_3, **2E**		*Z*-*n*-C_4H_3, **2Z**		**3**		**4**	
Ion state[a]	^{1}A' ($^1A_1$)	^{3}A" ($^3A_2$)	^{1}A' ($^1A_1$)[b]	^{3}A" (^{3}A")	^{1}A' ($^1A_1$)[c]	^{3}A" (^{3}A")	^{1}A' ($^1A_1$)[b]	^{3}A" (^{3}A")	^{1}A' ($^1A_1$)	^{3}A" (^{3}A")
VIE	8.46	9.84	9.77	9.85	9.79	9.87	9.45	9.00	8.25	8.57
AIE	8.01	9.63	7.51	9.70	8.30	9.70	6.69	8.67	7.39	8.21

[a]Electronic state of the cation at the geometry of the neutral C_4H_3 species and at the geometry optimized for the cation (in parentheses). [b]Geometry optimization of the cation converges to **1s$^+$**. [c]Geometry optimization of the cation converges to **4s$^+$**.

Having calculated the molecular structures of the C_4H_3 neutrals and their ions as well as the ionization energies and the inherent Franck Condon factors, we are turning our attention now to the experimental data obtained. Here, a scan of the photon energy allows for extraction of a photo-ionization efficiency (PIE) curve, which is shown in Figure 2. The signal originates at 8.0 eV, rises sharply up to about 8.2 eV and then plateaus out at about 8.7 eV; hereafter, the signal drops down to about 9.0 eV. From 9.0 eV on, the signal rises again to about 9.4 eV, decreases significantly until

9.6 eV, and rises once again very steeply to about 10.0 eV. These experimental data can be compared with simulated PIE curves (Figure 2). These simulated graphs are generated by convoluting the calculated FCFs with a 0.1 eV Gaussian function to simulate the light shape followed by integration. For the i-C_4H_3 isomer, the FCFs for different modes of the same energy were summed together. The red curve shows a simulation of equal contribution from isomer **1** and **4**, whereas the green curve represents a 90% contribution of isomer **1** and 10% contribution of isomer **4**. It is clear that the simulated PIE reproduces both the adiabatic onset and also the general slope of the experimental data up to 8.7 eV. Therefore, our data suggest the existence of both the acyclic and cyclic isomers **1** and **4**, respectively. Likewise, this section of the PIE curve correlates nicely with the computed AIE of the *i*-C_4H_3 structure of 8.01 eV versus the experimental onset of about 8.0 eV to yield the C_{2v} symmetric ion $\mathbf{1s^+}$ in its singlet state. As predicted theoretically, photoionization of isomer **4** leads to strong FCF intensities for the origin of $\mathbf{4t^+}$, but not to $\mathbf{4s^+}$. To summarize, the section of the PIE curve from 8.0 to 8.7 eV indicates the formation of an acyclic and cyclic C_4H_3 isomer in the supersonic beam: **1** and **4**. In a similar manner, the blue graph presents a simulated PIE curve for a 67% contribution from isomer **3** and 33% contribution from isomer **2E**; the magenta curve shows a contribution of 33% from the **2Z** isomer. Again it is apparent that the calculated PIEs broadly reproduce the shape of experimental PIE curve in the 9.0 eV to 10.0 eV region suggesting that isomer **3** as well as **2E/2Z** are present in the beam. Note that the dips at 9.0 eV and 9.7 eV are likely caused from auto ionization or from dissociative ionization of the precursors at higher photon energies. In the absence of absolute photoionization cross-sections, we shall stress that the assumed contributions of various isomers to the derived PIE allows for only a qualitative analysis of the population of isomers in the beam.

6. Conclusions

Our combined experimental and theoretical study suggested the synthesis of four C_4H_3 radicals in a supersonic beam generated via laser ablation of graphite and seeding the ablated species in neat methylacetylene, which also acted as a reagent. These are two acyclic radicals i-C_4H_3 [**1**] and E/Z-n-C_4H_3 [**2E/2Z**] and two cyclic structures **3** and **4**. Note that previous flame studies only suggested the formation of the thermodynamically most stable i-C_4H_3 isomer [9]. The different product spectra could be the result of a combination of distinct production methods of the radicals (supersonic be-

ams versus combustion flames) and different pressure conditions in the flame and within the supersonic expansion. Further, the present experiments support the prediction from previous crossed molecular beam studies of ground state carbon atom with methylacetylene at lower collision energies that a higher energy C_4H_3 isomer, possibly of cyclic structure, likely contributes to reactive scattering signal [11]. Theoretically, the reaction mechanism was suggested based on electronic structure calculations of the triplet C_4H_4 PES [25]. Upon reaction of laser ablated ground state carbon atoms, the latter could add to the carbon-carbon double bond of the methylacetylene molecule to form intermediates [i1], [i2], and/or [i3] (Figure 3). Structure [i1] could isomerize to [i2] via ring closure or undergoes hydrogen migration to [i4]. Alternatively, [i3] could ring-close to [i2] or [i5]; in the latter case the ring closure is accompanied with a 1,2-H shift. [i2] and [i5] could ring-open to yield [i4] and [i6], respectively. A hydrogen migration in [i4] can connect this structure to isomer [i6]. These intermediates can undergo unimolecular decomposition via atomic hydrogen loss to form the experimentally detected products **1** (from [i4] and [i6]), **2** (from [i6]), **3** (from [i2]), and **4** (from [i5]).

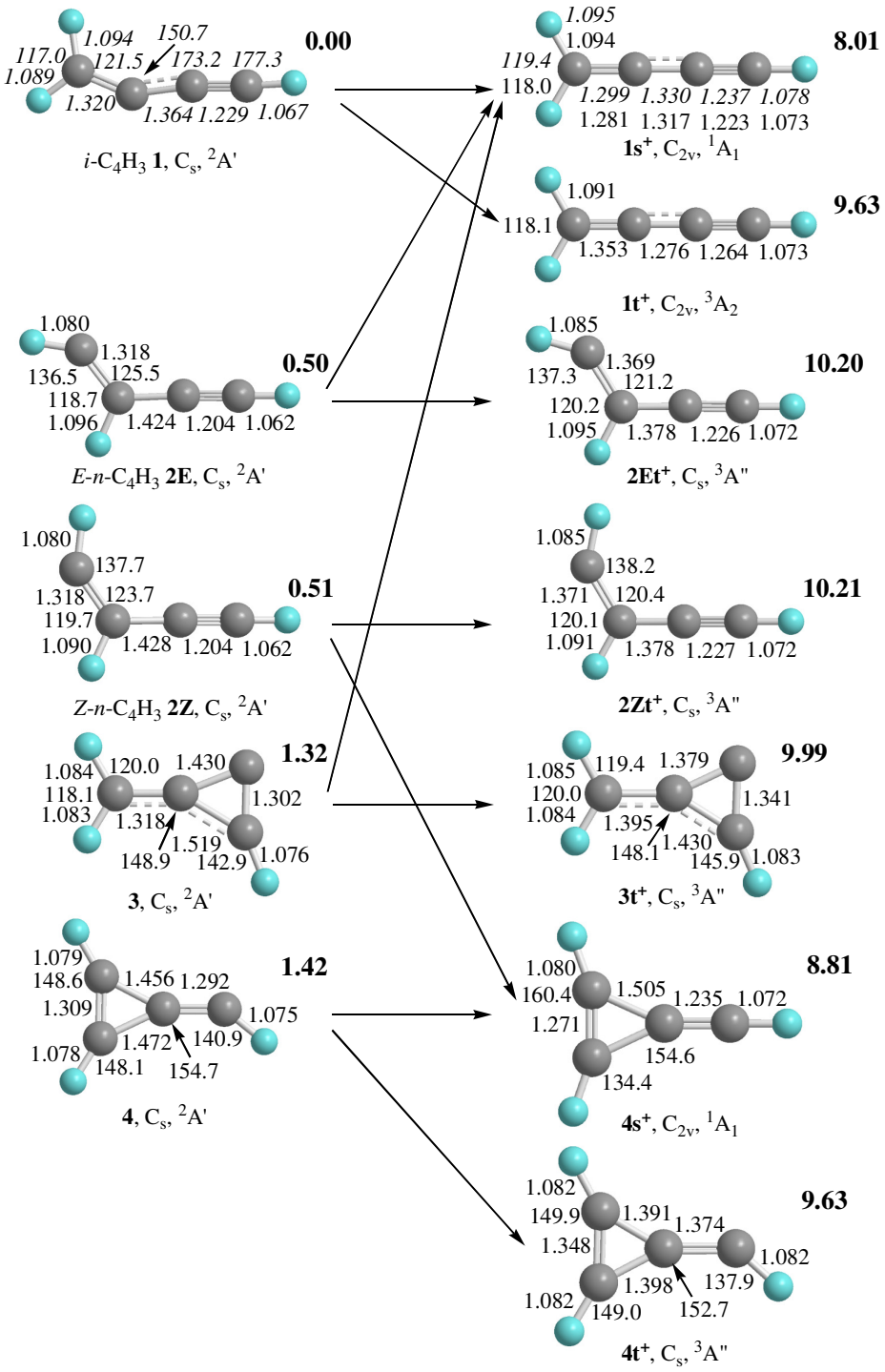

Figure 1. Geometries of neutral and ionic C_4H_3 isomers optimized at the B3LYP/6-311G** (plain numbers) and CCSD(T)/6-311G** (italics) levels of theory. Bond lengths are given in Angstrom and bond angles in degrees. Symmetry point groups and electronic states are also shown. Bold numbers give relative energies of the neutral and ionic species (in eV) with respect to *i*-C_4H_3 calculated at the CCSD(T)/CBS level of theory. Arrows show the directions of geometry relaxation after ionization.

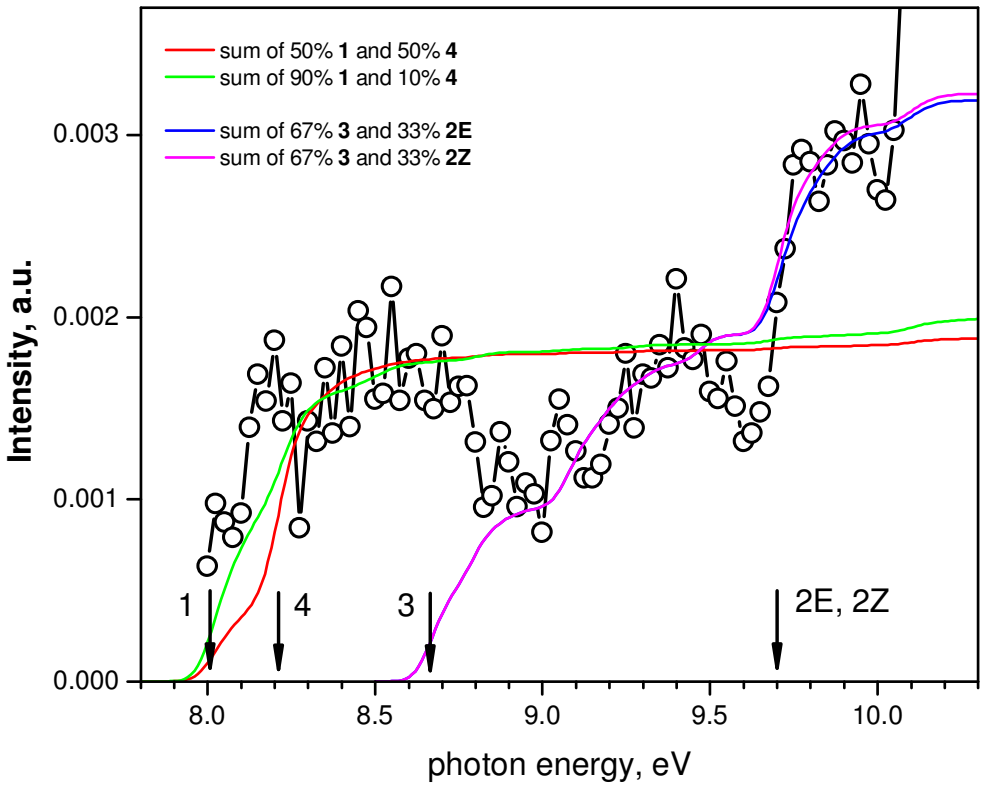

Figure 2. Photoionization efficiency curve for C_4H_3 isomers recorded at m/z = 51. Open circles correspond to experimental data. Arrows represent positions of calculated adiabatic ionization energies for various C_4H_3 isomers as compiled in Table 1.

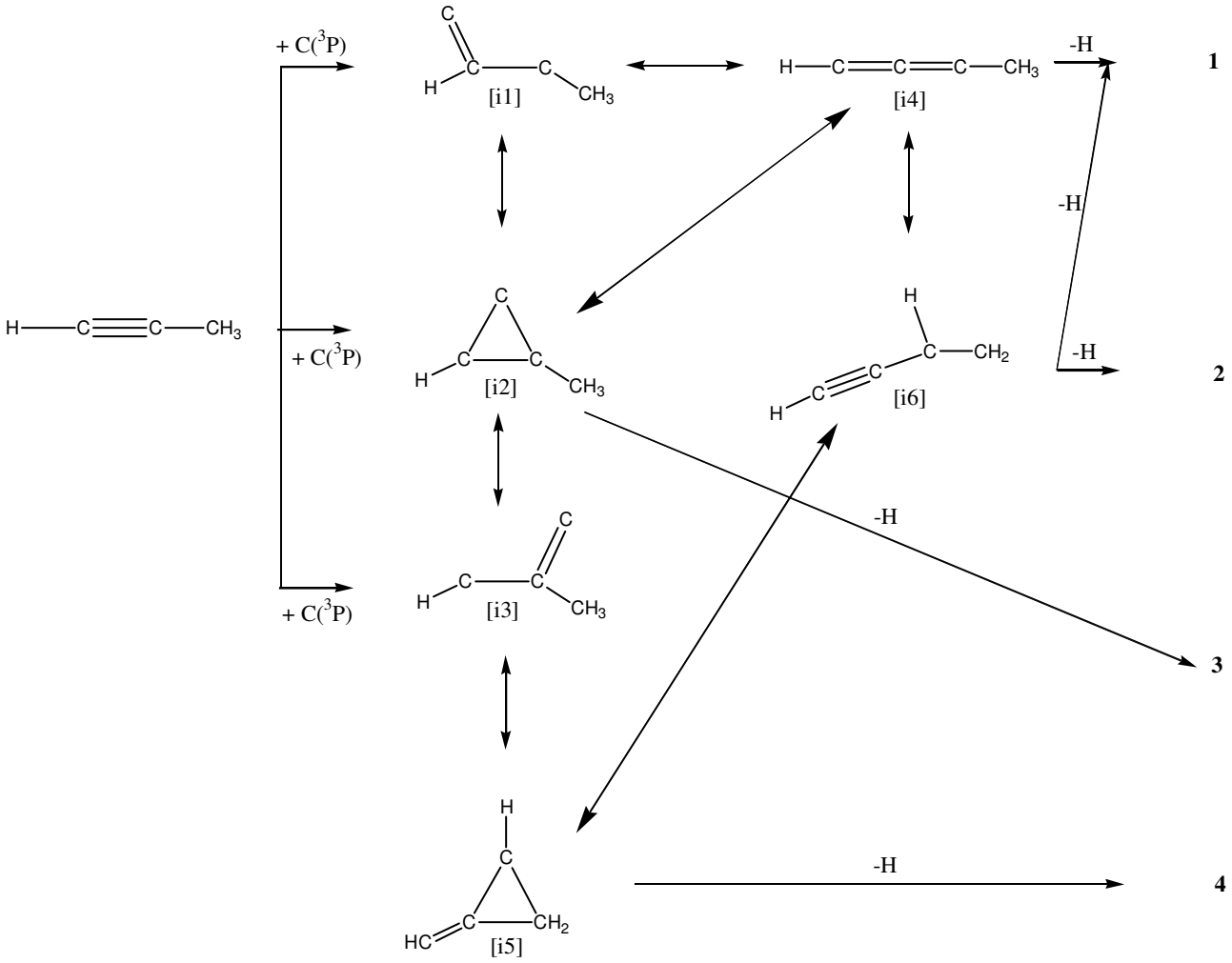

Figure 3. Schematic representation of the formation of four C_4H_3 isomers via reaction of ground state carbon atoms with methylacetylene, isomerization of the initial collision complexes, and decomposition of distinct intermediates to form multiple C_4H_3 structures.

Acknowledgments

This work was supported by the US Department of Energy, Basic Energy Sciences (DE-FG02-03ER15411 [RIK], DE-FG02-04ER15570 [AMM], and DE-AC02-05CH11231 [MA and OK]).

Keywords: combustion · astrochemistry · chemical dynamics · interstellar chemistry · ionization potentials · physical organic chemistry · reactive intermediates · resonantly stabilized free radicals

Supporting Information

Calculated Franck-Condon factors for C_4H_3 isomers

a) *i*-C_4H_3, **1s**$^+$($^1A_1$) ← **1**(^{2}A'). Individual Franck-Condon factors (FCF) characterizing the probability of excitation of single vibrational modes to a certain quantum number in the ion are presented. The energies of the corresponding vibronic peaks are given in eV and the frequencies of the active normal modes in the ion are in cm^{-1}. Overall FCFs can be computed as various possible products of individual FCFs; one individual FCF should be taken from each column.

Normal mode	ν_1'		ν_3'		ν_5'		ν_7'		ν_{11}'		ν_{12}'		ν_{15}'	
Ion's freq.	176		374		839		869		1789		2123		3380	
Vibrational quantum number	FCF	Energy	FCF	Energy	FCF	Energy	FCF	Energy	FCF	Energy	FCF	Energy	FCF	Energy
0	0.31	8.01	0.07	8.01	7.0E-10	8.01	0.26	8.01	0.43	8.01	0.24	8.01	0.00	8.01
1	0.36	8.03	0.20	8.05	1.2E-08	8.11	0.36	8.11	0.36	8.23	0.34	8.27	0.01	8.43
2	0.21	8.05	0.27	8.10	9.9E-08	8.22	0.24	8.22	0.15	8.45	0.24	8.53	0.02	8.85
3	0.09	8.07	0.23	8.15	5.8E-07	8.32	0.10	8.33	0.04	8.67	0.12	8.80	0.05	9.26
4	0.03	8.09	0.14	8.19	2.6E-06	8.42	0.03	8.44	0.01	8.89	0.04	9.06	0.09	9.68
5	0.01	8.12	0.06	8.24	9.4E-06	8.53	0.01	8.55			0.01	9.32	0.12	10.10
6			0.02	8.28	2.9E-05	8.63							0.15	10.52
7			0.01	8.33	8.0E-05	8.74							0.15	10.94
8					1.9E-04	8.84							0.13	11.36
9					4.3E-04	8.94							0.11	11.78
10					8.7E-04	9.05							0.07	12.20
11					1.6E-03	9.15							0.05	12.62
12					2.9E-03	9.26							0.03	13.04
13					4.7E-03	9.36							0.01	13.45
14					0.01	9.46							0.01	13.87
15					0.01	9.57								14.29

16	0.02	9.67
17	0.02	9.78
18	0.03	9.88
19	0.03	9.98
20	0.04	10.09
21	0.05	10.19
22	0.05	10.30
23	0.06	10.40
24	0.06	10.50
25	0.06	10.61
26	0.06	10.71
27	0.06	10.82
28	0.06	10.92
29	0.06	11.02
30	0.05	11.13
31	0.05	11.23
32	0.04	11.34
33	0.04	11.44
34	0.03	11.54
35	0.02	11.65
36	0.02	11.75
37	0.02	11.86
38	0.01	11.96
39	0.01	12.06
40	0.01	12.17
41	0.01	12.27

b) *E*-*n*-C_4H_3, **2Et**$^+$(^{3}A") ← **2E**(^{2}A'). Overall FCFs are given. The assignment shows vibrational quantum numbers for active normal modes in the ion: ν_1' (206 cm^{-1}), ν_6' (689 cm^{-1}), ν_{10}' (1244 cm^{-1}), and ν_{13}' (3067 cm^{-1}). The energies of the corresponding vibronic peaks are given in eV.

Assignment	FCF	Energy
Origin	0.41	9.70
ν_1' = 1	0.03	9.72
ν_6' = 1	0.18	9.78
ν_6' = 1, ν_1' = 1	0.01	9.81
ν_{10}' = 1	0.08	9.85
ν_6' = 2	0.04	9.87
ν_6' = 1, v10' = 1	0.03	9.94
ν_6' = 3	0.01	9.95
ν_{13}' = 1	0.09	10.08
ν_6' = 1, ν_{13}' = 1	0.04	10.16

c) *Z*-*n*-C_4H_3, **2Zt**$^+$(^{3}A") ← **2Z**(^{2}A'). Overall FCFs are given. The assignment shows vibrational quantum numbers for active normal modes in the ion: ν_1' (201 cm^{-1}), ν_5' (686 cm^{-1}), ν_{10}' (1254 cm^{-1}), ν_{13}' (3117 cm^{-1}), and ν_{14}' (3215 cm^{-1}). The energies of the corresponding vibronic peaks are given in eV.

Assignment	FCF	Energy
Origin	0.54	9.70
ν_1' = 1	0.01	9.73
ν_5' = 1	0.15	9.79
ν_5' = 1, ν_1' = 1	0.00	9.81
ν_{10}' = 1	0.07	9.86
ν_5' = 2	0.02	9.87
ν_5' = 1, ν_{10}' = 1	0.02	9.94
ν_{13}' = 1	0.07	10.09
ν_{14}' = 1	0.03	10.10
ν_5' = 1, ν_{13}' = 1	0.02	10.17

d) **3t**$^{+}$(^{3}A") ← **3**(^{2}A'). Overall FCFs are given. The assignment shows vibrational quantum numbers for active normal modes in the ion: ν_5' (837 cm^{-1}), ν_7' (938 cm^{-1}), ν_8' (1008 cm^{-1}), ν_9' (1143 cm^{-1}), ν_{12}' (1704 cm^{-1}), ν_{14}' (3255 cm^{-1}), and ν_{15}' (3243 cm^{-1}). The energies of the corresponding vibronic peaks are given in eV.

Assignment	FCF	Energy
Origin	0.175	8.67
ν_5' = 1	0.030	8.77
ν_7' = 1	0.023	8.78
ν_8' = 1	0.043	8.79
ν_9' = 1	0.040	8.81
ν_5' = 2	0.006	8.87
ν_{12}' = 1	0.016	8.88
ν_7' = 2	0.002	8.90
ν_8' = 2	0.007	8.92
ν_9' = 2	0.007	8.95
ν_{14}' = 1	0.120	9.07
ν_{15}' = 1	0.024	9.07
ν_{14}' = 1,ν_5' = 1	0.021	9.17
ν_{14}' = 1, ν_7' = 1	0.016	9.18
ν_{14}' = 1, ν_8' = 1	0.030	9.19
ν_{14}' = 1, ν_9' = 1	0.027	9.21
ν_{14}' = 1, ν_5' = 2	0.004	9.27
ν_{14}' = 1, ν_{12}' = 1	0.011	9.28
ν_{14}' = 1, ν_7' = 2	0.001	9.30
ν_{14}' = 1, ν_8' = 2	0.030	9.31
ν_{14}' = 1, ν_9' = 2	0.005	9.35
ν_{14}' = 1, ν_{15}' = 1	0.017	9.47
ν_{15}' = 2	0.002	9.47
ν_{14}' = 2	0.042	9.47
ν_{14}' = 1, ν_{15}' = 2	0.001	9.87
ν_{14}' = 3	0.010	9.88

e) **4t**$^{+}$(^{3}A") ← **4**(^{2}A'). Overall FCFs are given. The assignment shows vibrational quantum numbers for active normal modes in the ion: ν_1' (359cm^{-1}), ν_5' (796 cm^{-1}), ν_6' (862 cm^{-1}), ν_8' (1000 cm^{-1}), ν_9' (1019 cm^{-1}), ν_{10}' (1162 cm^{-1}), ν_{11}' (1420 cm^{-1}), ν_{12}' (1711 cm^{-1}), ν_{14}' (3269 cm^{-1}), and ν_{15}' (3243 cm^{-1}). The energies of the corresponding vibronic peaks are given in eV.

Assignment	FCF	Energy
Origin	0.752	8.21
ν_1' = 1	0.006	8.26
ν_5' = 1	0.018	8.31
ν_6' = 1	0.059	8.32
ν_8' = 1	0.017	8.34
ν_9' = 1	0.022	8.34
ν_{10}' = 1	0.026	8.36
ν_{11}' = 1	0.029	8.39
ν_5' = 2	0.003	8.41
ν_{12}' = 1	0.014	8.43
ν_6' = 2	0.006	8.43
ν_8' = 2	0.003	8.46
ν_{10}' = 2	0.002	8.50
ν_{14}' = 1	0.008	8.62
ν_{15}' = 1	0.006	8.62

[1] J.A. Miller, S.J. Klippenstein, *J. Phys. Chem. A* **2003**, 107, 7783.

[2] Y. Georgievskii, J.A. Miller, S.J. Klippenstein, *PCCP* **2007**, 9, 4259.

[3] A.M. Herring, J.T. McKinnon, D.E. Petrick, K.W. Gneshin, J. Filley, B.D. McCloskey, *Journal of Analytical and Applied Pyrolysis* **2003**, 66, 165.

[4] O. Morata, E. Herbst, *MNRAS* **2008**, 390, 1549.

[5] C. Boersma, A.L. Mattioda, C.W. Bauschlicher, E. Peeters, A.G.G.M. Tielens, L.J. Allamandola, *ApJ* **2009**, 690, 1208.

[6] T. Zhang, X.N. Tang, K.C. K.-C.; C.Y. Ng, C. Nicolas, D.S. Peterka, M. Ahmed, M.L. Morton, B. Ruscic, R. Yang, L.X. Wei, C.Q. Huang, B. Yang, J. Wang, L.S. Sheng, Y.W. Zhang, F. Qi, *JCP* **2006**, 124, 074302/1.

[7] J. Wang, U. Struckmeier, B. Yang, T.A. Cool, P. Osswald, K. Kohse-Hoinghaus, T. Kasper, N. Hansen, P.R. Westmoreland, *J. Phys. Chem. A* **2008**, 112, 9255.

[8] Y. Li, L. Zhang, Z. Tian, T. Yuan, J. Wang, B. Yang, F. Qi, Energy & Fuels **2009**, 23, 1473.

[9] N. Hansen, S.J. Klippenstein, C.A. Taatjes, J.A. Miller, J. Wang, T.A. Cool, B. Yang, R. Yang, L. Wei, C. Huang, J. Wang, F. Qi, *J. Phys. Chem. A* **2006**, 110, 3670.

[10] D. Domin, W.A. Lester, R. Whitesides, M. Frenklach, *J. Phys. Chem. A* **2008**, 112, 2065.

[11] R.I. Kaiser, D. Stranges, Y.T. Lee, A.G. Suits, *J. Chem. Phys.* **1996**, 105, 8721..

[12] R.I. Kaiser, A.M. Mebel, A.H.H. Chang, S.H. Lin, and Y.T. Lee, *J. Chem. Phys.* **1999**, 110, 10330.

[13] R.I. Kaiser, L. Belau, S.R. Leone, M. Ahmed, B. J. Braams, J. Bowman, *Chem. Phys. Chem.* **2007,** 8, 1236.

[14] A. D. Becke, *J. Chem. Phys*. **98**, 5648 (1993).

[15] C. Lee, W. Yang, and R. G. Parr, *Phys. Rev. B* **37**, 785 (1988).

[16] S. E. Wheeler, W. D. Allen, H. F. Schaefer III, *J. Chem. Phys*. **121**, 8800 (2004).

[17] T. N. Le, A. M. Mebel, R. I. Kaiser, *J. Comput. Chem*. **22**, 1522 (2001).

[18] G. D. Purvis and R. J. Bartlett, *J. Chem. Phys.* **76**, 1910 (1982); G. E. Scuseria, C. L. Janssen, and H. F. Schaefer, *III, J. Chem. Phys*. **89**, 7382 (1988); G. E. Scuseria, and H. F. Schaefer, III, *J. Chem. Phys.* 90, 3700 (1989); J. A. Pople, M. Head-Gordon, and K. Raghavachari, *J. Chem. Phys*. 87, 5968 (1987).

[19] T. H. Dunning, Jr., *J. Chem. Phys.* **90**, 1007 (1989).

[20] K. A. Peterson and T. H. Dunning, Jr., *J. Chem. Phys.* **99**, 3898 (1995).

[21] M. J. Frisch et al., Gaussian 98, Revision A.9; Gaussian, Inc.: Pittsburgh, PA, 1998.

[22] MOLPRO is a package of ab initio programs written by H.-J. Werner and P. J. Knowles with contributions from R. D. Amos et al., MOLPRO version 2002.6; University of Birmingham: Birmingham, UK, 2003.

[23] A. M. Mebel, Y.-T. Chen, S. H. Lin, *Chem. Phys. Lett.* **258**, 53 (1996).

[24] A. M. Mebel, Y.-T. Chen, S. H. Lin, *J. Chem. Phys.* **105**, 9007 (1996).

[25] A. M. Mebel, R. I. Kaiser, Y. T. Lee, *J. Am. Chem. Soc*. **122**, 1776 (2000).